Integer ambiguity resolution in precise point positioning: Method comparison

Article *in* Journal of Geodesy · September 2010

DOI: 10.1007/s00190-010-0399-x

CITATIONS
257

READS
2,132

4 authors:

J. Geng
Wuhan University
123 PUBLICATIONS **4,486** CITATIONS
SEE PROFILE

Xiaolin Meng
The Sino-UK Geospatial Engineering Centre; Global Geospatial Engineering Ltd.
263 PUBLICATIONS **4,932** CITATIONS
SEE PROFILE

Alan Dodson
University of Nottingham
132 PUBLICATIONS **4,227** CITATIONS
SEE PROFILE

Norman Teferle
University of Luxembourg
144 PUBLICATIONS **2,688** CITATIONS
SEE PROFILE

J Geod (2010) 84:569–581
DOI 10.1007/s00190-010-0399-x

ORIGINAL ARTICLE

Integer ambiguity resolution in precise point positioning: method comparison

Jianghui Geng · Xiaolin Meng · Alan H. Dodson · Felix N. Teferle

Received: 30 March 2010 / Accepted: 27 July 2010 / Published online: 6 August 2010

Abstract Integer ambiguity resolution at a single receiver can be implemented by applying improved satellite products where the fractional-cycle biases (FCBs) have been separated from the integer ambiguities in a network solution. One method to achieve these products is to estimate the FCBs by averaging the fractional parts of the float ambiguity estimates, and the other is to estimate the integer-recovery clocks by fixing the undifferenced ambiguities to integers in advance. In this paper, we theoretically prove the equivalence of the ambiguity-fixed position estimates derived from these two methods by assuming that the FCBs are hardware-dependent and only they are assimilated into the clocks and ambiguities. To verify this equivalence, we implement both methods in the Position and Navigation Data Analyst software to process 1 year of GPS data from a global network of about 350 stations. The mean biases between all daily position estimates derived from these two methods are only 0.2, 0.1 and 0.0 mm, whereas the standard deviations of all position differences are only 1.3, 0.8 and 2.0 mm for the East, North and Up components, respectively. Moreover, the differences of the position repeatabilities are below 0.2 mm on average for all three components. The RMS of the position estimates minus those from the International GNSS Service weekly solutions for the former method differs by below 0.1 mm on average for each component from that for the latter method. Therefore, considering the recognized millimeter-level precision of current GPS-derived daily positions, these statistics empirically demonstrate the theoretical equivalence of the ambiguity-fixed position estimates derived from these two methods. In practice, we note that the former method is compatible with current official clock-generation methods, whereas the latter method is not, but can potentially lead to slightly better positioning quality.

Keywords Precise point positioning · Ambiguity resolution · Fractional-cycle bias · Integer-recovery clock · Decoupled clock model

J. Geng (✉) · X. Meng · A. H. Dodson · F. N. Teferle
Institute of Engineering Surveying and Space Geodesy, University of Nottingham, Nottingham NG7 2TU, UK
e-mail: isxjg@nottingham.ac.uk

1 Introduction

Carrier-phase measurements of the Global Positioning System (GPS) suffer from the nuisance ambiguities which have to be estimated along with the other parameters of primary interest. Fortunately, integer resolutions of these ambiguities can be routinely performed for a network of receivers (e.g. Blewitt 2008). Fixing ambiguities to integers can significantly improve the positioning quality, especially for the East component (e.g. Blewitt 1989; Dong and Bock 1989), whereas keeping float ambiguities will potentially jeopardize the final solutions, such as introducing amplified spurious signals into the long-term position time series (e.g. King et al. 2003; Tregoning and Watson 2009).

Nonetheless, precise point positioning (PPP) (Zumberge et al. 1997) employs only one receiver, and thus its integer ambiguity resolution cannot be achieved simply following the methodology for the network solutions above. In fact, ambiguities in PPP are conventionally not fixed to integers. This is because the fractional-cycle biases (FCBs) in the GPS measurements are absorbed by the undifferenced ambiguity estimates and their integer properties are thus destroyed (Collins 2008; Ge et al. 2008; Mercier and Laurichesse 2008). In theory, these FCBs are presumed hardware-dependent, and present in all receivers and satellites (Teunissen and Kleusberg 1998). However, the temporal

property of the FCBs is not exactly known. Blewitt (1989) empirically reported that they were stable to better than 1 ns, whereas Gabor and Nerem (1999) simply assumed that they changed systematically with time. Despite this uncertainty, it is believed that the time-invariant parts of the FCBs cannot be separated from the undifferenced ambiguity estimates in the conventional PPP proposed by Zumberge et al. (1997), thus inhibiting the integer ambiguity resolution at a single receiver. Fortunately, a few recent studies have demonstrated that these integer resolutions can be achieved by applying improved satellite products where the FCBs have been separated from the integer ambiguities (Collins 2008; Ge et al. 2008; Laurichesse et al. 2009).

On the one hand, Ge et al. (2008) decomposed undifferenced ambiguities into wide-lane and narrow-lane ones, and applied the difference between satellites to remove the receiver-dependent FCBs. Utilizing a network of reference stations, wide-lane FCBs were determined by averaging the fractional parts of all pertinent wide-lane ambiguity estimates derived from the Melbourne–Wübbena combination measurements (Melbourne 1985; Wübbena 1985). Wide-lane FCBs are very stable over several days, or even a few months (Gabor and Nerem 1999). Similarly, narrow-lane FCBs were determined by averaging the fractional parts of all pertinent narrow-lane ambiguity estimates derived from the wide-lane ambiguities and the ionosphere-free-observable ambiguities. Due to the temporal instability of narrow-lane FCB estimates, their 15-min mean values were proposed to achieve high-precision solutions. At a single receiver, these wide-lane and narrow-lane FCBs were used to correct the ambiguity estimates to recover their integer properties. In practice, the daily positioning accuracy can be improved from 4.1, 3.1 and 8.3 mm to 2.8, 3.0 and 7.8 mm (Ge et al. 2008), whereas the hourly accuracy can be improved from 3.8, 1.5 and 2.8 cm to 0.5, 0.5, 1.4 cm for the East, North and Up components, respectively (Geng et al. 2009).

On the other hand, Laurichesse et al. (2009) applied the same decomposition, but directly fixed the undifferenced ambiguities to integers. Hence, an arbitrary value had to be assigned to the FCB of a specific receiver to obtain satellite-dependent FCBs. Their wide-lane FCB determination was the same as that of Ge et al. (2008). Nonetheless, the narrow-lane FCBs were not determined, but assimilated into the clock estimates. To achieve this by a network of reference stations, narrow-lane ambiguities had to be identified as integers and fixed to these integers before estimating the clocks. Similarly, Collins (2008) developed a decoupled clock model, characterized by pseudorange clocks differing from carrier-phase clocks. As narrow-lane ambiguities were fixed to integers before estimating the clocks, pseudorange measurements actually lost their indispensable role of separating clocks from ambiguities (Collins 2008), implying that pseudorange measurements could be ignored in estimating the carrier-phase clocks. Hence, we do not distinguish between the methods by Laurichesse et al. (2009) and Collins (2008), and name their carrier-phase clocks as the integer-recovery clocks (IRCs). At a single receiver, the IRCs were used to guarantee the integer properties of the narrow-lane ambiguities. In practice, the horizontal accuracy of epoch-wise position estimates at a static receiver was better than 2 cm (Laurichesse et al. 2009), and that of hourly position estimates was also better than 2 cm (Collins et al. 2008).

By contrasting the two methods above, we can find that their key difference is the strategy of separating the narrow-lane FCBs from the integer ambiguities. Ge et al. (2008) estimated the narrow-lane FCBs using float ambiguity estimates, whereas Laurichesse et al. (2009) assimilated the narrow-lane FCBs into the clock estimates. In this paper, we thus name the former method as FCB-based method, and the latter one as IRC-based method for brevity. From current publications, the positioning quality of the FCB-based method is close to that of the IRC-based method. In this case, of great interest is whether the ambiguity-fixed position estimates derived from these two methods coincide in theory and how they agree in practice.

Therefore, this paper aims at comparing the two methods above in both theory and practice. We will theoretically prove the equivalence between the ambiguity-fixed position estimates derived from these two methods, and then use one year of GPS data to illustrate how their daily position estimates agree in practice. In the following, Sect. 2 details the mathematical derivations for the equivalence of the ambiguity-fixed position estimates; Sect. 3 presents the data and models used in PPP; Sect. 4 examines the closeness between the daily positioning qualities; finally, Sect. 5 summarizes the main points of this paper and shows the perspectives of these two methods.

2 Theoretical analysis

Normally, ionosphere-free combination observables are used in PPP to eliminate the first-order ionospheric delays in the pseudorange and carrier-phase measurements. Hence, the linearized undifferenced measurement equations between receiver i and satellite k at a particular epoch are

$$\begin{cases} \Delta P_i^k = \mathbf{u}_i^k \Delta \mathbf{x}_i + c\Delta t_i^k + \lambda \left(b_i^k + \delta b_i^k\right) - e_i^k \\ \Delta L_i^k = \mathbf{u}_i^k \Delta \mathbf{x}_i + c\Delta t_i^k + \lambda \left(B_i^k + \delta B_i^k\right) + \lambda \Delta N_i^k - \varepsilon_i^k \end{cases} \tag{1}$$

where ΔP_i^k and ΔL_i^k denote the observed minus computed measurements for the pseudorange and carrier-phase, respectively; $\mathbf{u}_i^k$ contains the unit vector from the satellite to the receiver and the mapping function of the zenith tropospheric delay (ZTD); $\Delta \mathbf{x}_i^k$ contains the increments for the a priori

receiver position vector and ZTD; c denotes the light speed; λ denotes the narrow-lane wavelength, and thus following "FCBs" represent "narrow-lane FCBs" for brevity except when otherwise noted; $\Delta t_i^k = \Delta t_i - \Delta t^k$ where Δt_i and Δt^k denote the increments for the a priori receiver and satellite clocks, respectively; $B_i^k + \delta B_i^k$ is the carrier-phase FCB where B_i^k denotes the constant offset, i.e. the time-invariant part, and δB_i^k denotes the time-dependent deviation from B_i^k; $B_i^k = B_i - B^k$ and $\delta B_i^k = \delta B_i - \delta B^k$ where B_i and δB_i are for the receiver whereas B^k and δB^k are for the satellite; similarly, $b_i^k + \delta b_i^k$ is the fractional-cycle part of the pseudorange bias which is hereafter called pseudorange FCB for convenience; note that integer-cycle biases do not affect the integer properties of ambiguities, and are ignored throughout this study; ΔN_i^k denotes the integer increments of the a priori narrow-lane ambiguity; finally, e_i^k and ε_i^k denote the residual errors of the pseudorange and carrier-phase measurements, respectively (Teunissen and Kleusberg 1998). We note that the wide-lane ambiguity should be estimated before an integer narrow-lane ΔN_i^k can be introduced into Eq. 1 (see Appendix).

From Eq. 1, if receiver i observes m satellites at a particular epoch, we can obtain

$$\begin{bmatrix} e_i^1 \\ \vdots \\ e_i^m \\ \varepsilon_i^1 \\ \vdots \\ \varepsilon_i^m \end{bmatrix} = \begin{bmatrix} \mathbf{u}_i^1 & c\mathbf{I}^1 & \lambda\mathbf{I}^1 & \lambda\mathbf{I}^1 & \mathbf{0} & \mathbf{0} & \mathbf{0} \\ \vdots & \vdots & \vdots & \vdots & \vdots & \vdots & \vdots \\ \mathbf{u}_i^m & c\mathbf{I}^m & \lambda\mathbf{I}^m & \lambda\mathbf{I}^m & \mathbf{0} & \mathbf{0} & \mathbf{0} \\ \mathbf{u}_i^1 & c\mathbf{I}^1 & \mathbf{0} & \mathbf{0} & \lambda\mathbf{I}^1 & \lambda\mathbf{I}^1 & \lambda\mathbf{I}^1 \\ \vdots & \vdots & \vdots & \vdots & \vdots & \vdots & \vdots \\ \mathbf{u}_i^m & c\mathbf{I}^m & \mathbf{0} & \mathbf{0} & \lambda\mathbf{I}^m & \lambda\mathbf{I}^m & \lambda\mathbf{I}^m \end{bmatrix} \times \begin{bmatrix} \Delta\mathbf{x}_i \\ \Delta\mathbf{t}_i \\ \mathbf{b}_i \\ \delta\mathbf{b}_i \\ \mathbf{B}_i \\ \delta\mathbf{B}_i \\ \Delta\mathbf{N}_i \end{bmatrix} - \begin{bmatrix} \Delta P_i^1 \\ \vdots \\ \Delta P_i^m \\ \Delta L_i^1 \\ \vdots \\ \Delta L_i^m \end{bmatrix} \tag{2}$$

where $\mathbf{I}^h$ denotes an m-dimensional row-vector of which the hth element is 1 while all others are 0 ($h = 1, \ldots, m$); $\mathbf{0}$ denotes an m-dimensional zero row-vector; finally, each of $\Delta\mathbf{t}_i$, $\mathbf{b}_i$, $\delta\mathbf{b}_i$, $\mathbf{B}_i$, $\delta\mathbf{B}_i$ and $\Delta\mathbf{N}_i$ denotes an m-dimensional column-vector corresponding to m satellites, $\Delta\mathbf{t}_i = \left[\Delta t_i^1, \ldots, \Delta t_i^m\right]^{\mathrm{T}}$ for example. All unknown parameters except $\Delta\mathbf{x}_i$ are linearly correlated, hence preventing them from being simultaneously estimated in a least squares adjustment.

In fact, only $\Delta\mathbf{x}_i$, $\Delta\mathbf{t}_i$ and $\Delta\mathbf{N}_i$ are taken as to-be-estimated parameters in PPP. Hence, after a least squares adjustment, all $\mathbf{b}_i$, $\delta\mathbf{b}_i$, $\mathbf{B}_i$ and $\delta\mathbf{B}_i$ should finally be assimilated into $\Delta\mathbf{t}_i$ and $\Delta\mathbf{N}_i$, or otherwise into the residuals, namely the left side of Eq. 2. Such an assimilation should rigorously satisfy the requirement of minimizing the weighted sum squares of residuals. Under the constraint of this rule, we derive these assimilations by applying elementary column transformations (Meyer 2000) to Eq. 2 and conclude what the FCB and IRC estimates theoretically contain after a network solution. Note that our assumption for this theoretical analysis is that FCBs are hardware-dependent and only they are assimilated into the to-be-estimated parameters whilst all e_i^k and ε_i^k add to the residuals.

Then, we apply these theoretical FCB and IRC estimates to a single-receiver solution and finally achieve identical ambiguity-fixed position estimates for these two methods. To simplify the formula derivation, we apply the difference between satellites on Eq. 2 to avoid considering the receiver clocks and the receiver-dependent FCBs. Note that this operation does not affect the estimates of $\Delta\mathbf{x}_i$. More importantly, in this case, we can ignore the pseudorange measurements because we do not need them to separate the clocks and the ambiguities. Moreover, satellite clocks are precisely known and thus should be moved to the observed minus computed measurements. Hence,

$$\begin{bmatrix} \varepsilon_i^{2,1} \\ \vdots \\ \varepsilon_i^{m,1} \end{bmatrix} = \begin{bmatrix} \mathbf{u}_i^{2,1} & -\lambda\mathbf{I}^1 & -\lambda\mathbf{I}^1 & \lambda\mathbf{I}^1 \\ \vdots & \vdots & \vdots & \vdots \\ \mathbf{u}_i^{m,1} & -\lambda\mathbf{I}^{m-1} & -\lambda\mathbf{I}^{m-1} & \lambda\mathbf{I}^{m-1} \end{bmatrix} \begin{bmatrix} \Delta\mathbf{x}_i \\ \dot{\mathbf{B}} \\ \delta\dot{\mathbf{B}} \\ \Delta\dot{\mathbf{N}}_i \end{bmatrix} - \begin{bmatrix} \Delta L_i^{2,1} + c\Delta t^{2,1} \\ \vdots \\ \Delta L_i^{m,1} + c\Delta t^{m,1} \end{bmatrix} \tag{3}$$

where $\mathbf{I}^h$ is now an $(m-1)$-dimensional row-vector; $\dot{\mathbf{B}} = \left[B^{2,1}, \cdots B^{m,1}\right]^{\mathrm{T}}$, $\delta\dot{\mathbf{B}} = \left[\delta B^{2,1}, \cdots \delta B^{m,1}\right]^{\mathrm{T}}$ and $\Delta\dot{\mathbf{N}}_i = \left[\Delta N_i^{2,1}, \cdots \Delta N_i^{m,1}\right]^{\mathrm{T}}$ where the superscript for each vector element denotes the difference between satellites. In the following, we first derive the FCBs and IRCs using Eq. 2 and then derive the ambiguity-fixed position estimates using Eq. 3.

2.1 Fractional-cycle bias determination and ambiguity-fixed position estimates

In order to determine FCBs, we have to derive what a narrow-lane ambiguity estimate theoretically contains after a least squares adjustment. As demonstrated by Defraigne and Bruyninx (2007), biases in the pseudorange measurements

govern the absolute clock offsets generated in the conventional PPP. Hence in Eq. 2, the pseudorange time-invariant FCBs $\mathbf{b}_i$ should be assimilated into the clocks. For the carrier-phase measurements, offsets of $\mathbf{b}_i$ are thus introduced by the pseudorange-based clocks, and are finally assimilated into the integer ambiguities together with the carrier-phase time-invariant FCBs $\mathbf{B}_i$, namely

$$\begin{bmatrix} e_i^1 \\ \vdots \\ e_i^m \\ \varepsilon_i^1 \\ \vdots \\ \varepsilon_i^m \end{bmatrix} = \begin{bmatrix} \mathbf{u}_i^1 & c\mathbf{I}^1 & \lambda\mathbf{I}^1 & \mathbf{0} & \mathbf{0} \\ \vdots & \vdots & \vdots & \vdots & \vdots \\ \mathbf{u}_i^m & c\mathbf{I}^m & \lambda\mathbf{I}^m & \mathbf{0} & \mathbf{0} \\ \mathbf{u}_i^1 & c\mathbf{I}^1 & \mathbf{0} & \lambda\mathbf{I}^1 & \lambda\mathbf{I}^1 \\ \vdots & \vdots & \vdots & \vdots & \vdots \\ \mathbf{u}_i^m & c\mathbf{I}^m & \mathbf{0} & \lambda\mathbf{I}^m & \lambda\mathbf{I}^m \end{bmatrix} \times \begin{bmatrix} \Delta\mathbf{x}_i \\ \Delta\mathbf{t}_i + \frac{\lambda}{c}\mathbf{b}_i \\ \delta\mathbf{b}_i \\ \delta\mathbf{B}_i \\ \Delta\mathbf{N}_i + \mathbf{B}_i - \mathbf{b}_i \end{bmatrix} - \begin{bmatrix} \Delta P_i^1 \\ \vdots \\ \Delta P_i^m \\ \Delta L_i^1 \\ \vdots \\ \Delta L_i^m \end{bmatrix} \tag{4}$$

Note that the residuals are not changed. Conversely, if it is the carrier-phase time-invariant FCBs $\mathbf{B}_i$ that are assimilated into the clocks, the resulting offsets $\mathbf{B}_i$ in the pseudorange measurements then have to be assimilated into the pseudorange residuals, consequently enlarging the weighted sum squares of residuals. This apagogically proves the manner in which time-invariant FCBs are assimilated into the clocks and ambiguities, as illustrated by Eq. 4.

On the other hand, time-dependent FCBs can be assimilated only into the clocks. However, the residuals have to be enlarged because the pseudorange and carrier-phase FCBs differ. Due to the far-weak weights posed on pseudorange measurements, the carrier-phase FCBs $\delta\mathbf{B}_i$, rather than the pseudorange FCBs $\delta\mathbf{b}_i$, should be assimilated into the clocks and all remaining FCBs are assimilated into the pseudorange residuals, namely

$$\begin{bmatrix} e_i^1 - \lambda\delta b_i^1 + \lambda\delta B_i^1 \\ \vdots \\ e_i^m - \lambda\delta b_i^m + \lambda\delta B_i^m \\ \varepsilon_i^1 \\ \vdots \\ \varepsilon_i^m \end{bmatrix} = \begin{bmatrix} \mathbf{u}_i^1 & c\mathbf{I}^1 & \mathbf{0} \\ \vdots & \vdots & \vdots \\ \mathbf{u}_i^m & c\mathbf{I}^m & \mathbf{0} \\ \mathbf{u}_i^1 & c\mathbf{I}^1 & \lambda\mathbf{I}^1 \\ \vdots & \vdots & \vdots \\ \mathbf{u}_i^m & c\mathbf{I}^m & \lambda\mathbf{I}^m \end{bmatrix} \times \begin{bmatrix} \Delta\mathbf{x}_i \\ \Delta\mathbf{t}_i + \frac{\lambda}{c}\mathbf{b}_i + \frac{\lambda}{c}\delta\mathbf{B}_i \\ \Delta\mathbf{N}_i + \mathbf{B}_i - \mathbf{b}_i \end{bmatrix} - \begin{bmatrix} \Delta P_i^1 \\ \vdots \\ \Delta P_i^m \\ \Delta L_i^1 \\ \vdots \\ \Delta L_i^m \end{bmatrix} \tag{5}$$

Conversely, if it is $\delta\mathbf{b}_i$ that are assimilated into the clocks, the resulting offsets $\delta\mathbf{b}_i$ in the carrier-phase measurements then have to be assimilated into the highly weighted carrier-phase residuals, consequently enlarging the weighted sum squares of residuals more significantly than Eq. 5. This again apagogically justifies the derivation of Eq. 5. Note that the unknowns in Eq. 5 should be estimated using a network of reference stations.

From Eq. 5, we can derive that $\Delta\mathbf{t}_i + \frac{\lambda}{c}\mathbf{b}_i + \frac{\lambda}{c}\delta\mathbf{B}_i$ are the estimated increments for the a priori clocks, whereas $\Delta\mathbf{N}_i + \mathbf{B}_i - \mathbf{b}_i$ are the estimated float increments for the a priori integer ambiguities. The clock estimates should be divided into the receiver and satellite clocks by constraining a receiver clock to zero or the sum of a clock ensemble to zero. Hence, the clock estimate for a specific satellite k can be written as $\Delta t^k + \frac{\lambda}{c}b^k + \frac{\lambda}{c}\delta B^k$. In practice, an unknown bias should be present in this satellite clock estimate, but fortunately this bias is identical for all satellite clocks and can be absorbed by the receiver clock in a single-receiver solution without impairing the position estimate. Furthermore, we difference the ambiguity estimates between the kth and the first satellites and obtain $\Delta N_i^{k,1} + b^{k,1} - B^{k,1}$ $(k = 2, \ldots, m)$. For convenience, we presume that $b^{k,1} - B^{k,1}$ is still fractional. After removing $\Delta N_i^{k,1}$ by an integer rounding, we finally obtain the FCB estimates for satellite pairs, namely $b^{k,1} - B^{k,1}$. Note that we used to name these satellite-pair FCBs as uncalibrated hardware or phase delays in previous publications (Geng et al. 2009, 2010a,b,c).

At a single receiver, the above satellite clock and satellite-pair FCB estimates are applied to Eq. 3 in order to achieve ambiguity-fixed position estimates. Note that $\Delta t^{k,1}$ in Eq. 3 should be replaced by $\Delta t^{k,1} + \frac{\lambda}{c}b^{k,1} + \frac{\lambda}{c}\delta B^{k,1}$. As a result, $\delta\dot{\mathbf{B}}$ can be removed from the parameter vector in Eq. 3 because they have been corrected by the satellite clocks, but $\dot{\mathbf{b}}$ has to be inserted because the satellite clocks introduce additional errors of $\dot{\mathbf{b}}$, namely

$$\begin{bmatrix} \varepsilon_i^{2,1} \\ \vdots \\ \varepsilon_i^{m,1} \end{bmatrix} = \begin{bmatrix} \mathbf{u}_i^{2,1} & \lambda\mathbf{I}^1 & -\lambda\mathbf{I}^1 & \lambda\mathbf{I}^1 \\ \vdots & \vdots & \vdots & \vdots \\ \mathbf{u}_i^{m,1} & \lambda\mathbf{I}^{m-1} & -\lambda\mathbf{I}^{m-1} & \lambda\mathbf{I}^{m-1} \end{bmatrix} \begin{bmatrix} \Delta\mathbf{x}_i \\ \dot{\mathbf{b}} \\ \dot{\mathbf{B}} \\ \Delta\dot{\mathbf{N}}_i \end{bmatrix}$$

$$-\begin{bmatrix} \Delta L_i^{2,1} + c\Delta t^{2,1} + \lambda b^{2,1} + \lambda\delta B^{2,1} \\ \vdots \\ \Delta L_i^{m,1} + c\Delta t^{m,1} + \lambda b^{m,1} + \lambda\delta B^{m,1} \end{bmatrix} \tag{6}$$

where $\dot{\mathbf{b}} = \left[b^{2,1}, \ldots, b^{m,1}\right]^{\mathrm{T}}$. Furthermore, similar to Eq. 4, Eq. 6 actually becomes

$$\begin{bmatrix} \varepsilon_i^{2,1} \\ \vdots \\ \varepsilon_i^{m,1} \end{bmatrix} = \begin{bmatrix} \mathbf{u}_i^{2,1} & \lambda\mathbf{I}^1 \\ \vdots & \vdots \\ \mathbf{u}_i^{m,1} & \lambda\mathbf{I}^{m-1} \end{bmatrix} \begin{bmatrix} \Delta\mathbf{x}_i \\ \Delta\dot{\mathbf{N}}_i + \dot{\mathbf{b}} - \dot{\mathbf{B}} \end{bmatrix} - \begin{bmatrix} \Delta L_i^{2,1} + c\Delta t^{2,1} + \lambda b^{2,1} + \lambda\delta B^{2,1} \\ \vdots \\ \Delta L_i^{m,1} + c\Delta t^{m,1} + \lambda b^{m,1} + \lambda\delta B^{m,1} \end{bmatrix} \tag{7}$$

From Eq. 7, if the resulting float ambiguity estimate $\Delta N_i^{k,1} + b^{k,1} - B^{k,1}$ is corrected by the satellite-pair FCB $b^{k,1} - B^{k,1}$, we can attempt to fix the resulting $\Delta N_i^{k,1}$ to an integer. If this integer resolution succeeds, the unknown parameters contain only $\Delta\mathbf{x}_i$ and hence we deduct the fixed ambiguities from the observed minus computed measurements, namely

$$\begin{bmatrix} \varepsilon_i^{2,1} \\ \vdots \\ \varepsilon_i^{m,1} \end{bmatrix} = \begin{bmatrix} \mathbf{u}_i^{2,1} \\ \vdots \\ \mathbf{u}_i^{m,1} \end{bmatrix} \left[\Delta\mathbf{x}_i\right] - \begin{bmatrix} \Delta L_i^{2,1} - \lambda\Delta N_i^{2,1} + c\Delta t^{2,1} + \lambda B^{2,1} + \lambda\delta B^{2,1} \\ \vdots \\ \Delta L_i^{m,1} - \lambda\Delta N_i^{m,1} + c\Delta t^{m,1} + \lambda B^{m,1} + \lambda\delta B^{m,1} \end{bmatrix} \tag{8}$$

Equation 8 is then used to estimate the ambiguity-fixed $\Delta\mathbf{x}_i$ according to the theory of least squares adjustment. Note that Eq. 8 is actually for epoch-wise positioning, but multi-epoch positioning can be easily derived by superimposing Eq. 8.

2.2 Integer-recovery clock determination and ambiguity-fixed position estimates

In order to determine IRCs, we first have to identify the undifferenced ambiguities as integers in a network solution. In Eq. 2, if we successfully fix $\Delta\mathbf{N}_i$ to integers, $\Delta\mathbf{N}_i$ can then be removed from the parameter vector and deducted from the observed minus computed measurements, namely

$$\begin{bmatrix} e_i^1 \\ \vdots \\ e_i^m \\ \varepsilon_i^1 \\ \vdots \\ \varepsilon_i^m \end{bmatrix} = \begin{bmatrix} \mathbf{u}_i^1 & c\mathbf{I}^1 & \lambda\mathbf{I}^1 & \lambda\mathbf{I}^1 & \mathbf{0} & \mathbf{0} \\ \vdots & \vdots & \vdots & \vdots & \vdots & \vdots \\ \mathbf{u}_i^m & c\mathbf{I}^m & \lambda\mathbf{I}^m & \lambda\mathbf{I}^m & \mathbf{0} & \mathbf{0} \\ \mathbf{u}_i^1 & c\mathbf{I}^1 & \mathbf{0} & \mathbf{0} & \lambda\mathbf{I}^1 & \lambda\mathbf{I}^1 \\ \vdots & \vdots & \vdots & \vdots & \vdots & \vdots \\ \mathbf{u}_i^m & c\mathbf{I}^m & \mathbf{0} & \mathbf{0} & \lambda\mathbf{I}^m & \lambda\mathbf{I}^m \end{bmatrix} \begin{bmatrix} \Delta\mathbf{x}_i \\ \Delta\mathbf{t}_i \\ \mathbf{b}_i \\ \delta\mathbf{b}_i \\ \mathbf{B}_i \\ \delta\mathbf{B}_i \end{bmatrix} - \begin{bmatrix} \Delta P_i^1 \\ \vdots \\ \Delta P_i^m \\ \Delta L_i^1 - \lambda\Delta N_i^1 \\ \vdots \\ \Delta L_i^m - \lambda\Delta N_i^m \end{bmatrix} \tag{9}$$

Then similar to Eq. 5, the carrier-phase FCBs $\mathbf{B}_i + \delta\mathbf{B}_i$, rather than the pseudorange FCBs $\mathbf{b}_i + \delta\mathbf{b}_i$, are assimilated into the clocks. The resulting offsets $\mathbf{B}_i + \delta\mathbf{B}_i$ in the pseudorange measurements have to be assimilated into the pseudorange residuals together with $\mathbf{b}_i + \delta\mathbf{b}_i$. Hence, Eq. 9 becomes

$$\begin{bmatrix} e_i^1 - \lambda b_i^1 - \lambda\delta b_i^1 + \lambda B_i^1 + \lambda\delta B_i^1 \\ \vdots \\ e_i^m - \lambda b_i^m - \lambda\delta b_i^m + \lambda B_i^m + \lambda\delta B_i^m \\ \varepsilon_i^1 \\ \vdots \\ \varepsilon_i^m \end{bmatrix} = \begin{bmatrix} \mathbf{u}_i^1 & c\mathbf{I}^1 \\ \vdots & \vdots \\ \mathbf{u}_i^m & c\mathbf{I}^m \\ \mathbf{u}_i^1 & c\mathbf{I}^1 \\ \vdots & \vdots \\ \mathbf{u}_i^m & c\mathbf{I}^m \end{bmatrix} \times \begin{bmatrix} \Delta\mathbf{x}_i \\ \Delta\mathbf{t}_i + \dfrac{\lambda}{c}\mathbf{B}_i + \dfrac{\lambda}{c}\delta\mathbf{B}_i \end{bmatrix} - \begin{bmatrix} \Delta P_i^1 \\ \vdots \\ \Delta P_i^m \\ \Delta L_i^1 - \lambda\Delta N_i^1 \\ \vdots \\ \Delta L_i^m - \lambda\Delta N_i^m \end{bmatrix} \tag{10}$$

Again, the unknowns in Eq. 10 should be estimated using a network of reference stations. Hence, IRCs are equal to $\Delta\mathbf{t}_i + \dfrac{\lambda}{c}\mathbf{B}_i + \dfrac{\lambda}{c}\delta\mathbf{B}_i$ plus the a priori clocks. The IRC for a specific satellite k can be written as $\Delta t^k + \frac{\lambda}{c}B^k + \frac{\lambda}{c}\delta B^k$.

At a single receiver, the above satellite IRCs are applied to Eq. 3 in order to achieve ambiguity-fixed position estimates. Note that $\Delta t^{k,1}$ in Eq. 3 should be replaced by $\Delta t^{k,1} + \frac{\lambda}{c} B^{k,1} + \frac{\lambda}{c}\delta B^{k,1}$. As a result, both $\dot{\mathbf{B}}$ and $\delta\dot{\mathbf{B}}$ are removed from the parameter vector in Eq. 3 because they have been corrected by the satellite clocks, namely

$$\begin{bmatrix} \varepsilon_i^{2,1} \\ \vdots \\ \varepsilon_i^{m,1} \end{bmatrix} = \begin{bmatrix} \mathbf{u}_i^{2,1} & \lambda\mathbf{I}^1 \\ \vdots & \vdots \\ \mathbf{u}_i^{m,1} & \lambda\mathbf{I}^{m-1} \end{bmatrix} \begin{bmatrix} \Delta\mathbf{x}_i \\ \Delta\dot{\mathbf{N}}_i \end{bmatrix} - \begin{bmatrix} \Delta L_i^{2,1} + c\Delta t^{2,1} + \lambda B^{2,1} + \lambda\delta B^{2,1} \\ \vdots \\ \Delta L_i^{m,1} + c\Delta t^{m,1} + \lambda B^{m,1} + \lambda\delta B^{m,1} \end{bmatrix} \tag{11}$$

Then, if $\Delta\dot{\mathbf{N}}_i$ can be successfully fixed to integers, they can be deducted from the observed minus computed measurements and Eq. 11 becomes

$$\begin{bmatrix} \varepsilon_i^{2,1} \\ \vdots \\ \varepsilon_i^{m,1} \end{bmatrix} = \begin{bmatrix} \mathbf{u}_i^{2,1} \\ \vdots \\ \mathbf{u}_i^{m,1} \end{bmatrix} \left[\Delta\mathbf{x}_i \right] - \begin{bmatrix} \Delta L_i^{2,1} - \lambda\Delta N_i^{2,1} + c\Delta t^{2,1} + \lambda B^{2,1} + \lambda\delta B^{2,1} \\ \vdots \\ \Delta L_i^{m,1} - \lambda\Delta N_i^{m,1} + c\Delta t^{m,1} + \lambda B^{m,1} + \lambda\delta B^{m,1} \end{bmatrix}. \tag{12}$$

2.3 Remarks on the equivalence of ambiguity-fixed position estimates

By contrasting Eqs. 8 and 12, we can find that their design matrices and observed minus computed measurements are exactly the same, which demonstrates that the resulting estimates for $\Delta\mathbf{x}_i$ from the FCB-based and IRC-based methods should also be identical. This equivalence implies that a systematic difference between the $\Delta\mathbf{x}_i$ estimates in practice, if existing, should not be caused by the differences of the two methods themselves. Ideally, the difference between the actual $\Delta\mathbf{x}_i$ estimates should be minimal and random in nature. Additionally, in terms of Eq. 1, $\Delta\mathbf{x}_i$ also contains ZTD. Hence, identical ZTD estimates can also be achieved using these two methods. Note that this theoretical equivalence is derived from Eq. 2, namely the linearized measurement equation, thereby implying that identical models should be employed to reduce the raw measurements in order to achieve identical $\Delta\mathbf{x}_i$ estimates.

Nevertheless, this equivalence is largely based on our assumption that only the hardware-dependent FCBs are assimilated into the clock and undifferenced ambiguity estimates, which is not true in practice. Ge et al. (2008) illustrated that satellite-pair FCB estimates change temporally and spatially, and the fluctuation magnitude can reach up to 0.4 cycles, showing that these FCB estimates are contaminated by unknown temporally- and spatially correlated errors, such as the inaccurate modeling of tropospheric delays. This explains why FCB estimates are not constant values in practice. Likewise, actual IRC estimates are likely to absorb not only the hardware-dependent FCBs, but also some unknown common errors among a network of stations. We stress that these unknown redundant errors are not hardware-dependent, and thus they are likely to change under different distributions of reference stations. In the following sections, "FCB estimates" thus also contain these redundant errors.

Furthermore, from the observed minus computed measurements in Eqs. 8 and 12, $\Delta t^{k,1} + \frac{\lambda}{c} B^{k,1} + \frac{\lambda}{c}\delta B^{k,1}$ ($k = 2, \ldots, m$) can actually be taken as the satellite clock that can assist retrieving integer ambiguities. In the FCB-based method, this clock is finally achieved by combining the satellite clock estimate and the FCB estimate. Comparatively, this clock is exactly the IRC in the IRC-based method. This difference is attributed to the different strategies of separating FCBs from integer ambiguities in these two methods. Specifically, this separation is performed at the ambiguity-estimate level in the FCB-based method, whereas at the measurement-modeling level in the IRC-based method. As a result, the composition of redundant errors can be significantly different between the actual IRC estimates and the actual FCB estimates plus their corresponding satellite clock estimates, finally leading to different $\Delta\mathbf{x}_i$ estimates.

3 Data processing

One year of daily GPS data at about 350 globally distributed reference stations from the International GNSS Service (IGS) permanent network in 2008 were used (Dow et al. 2009). We removed those data files covering less than 6 h of measurements. Moreover, Center for Orbit Determination in Europe (CODE) final satellite orbits, 30-s satellite clocks, Earth rotation parameters (ERPs) and P1-C1 differential code biases were used (Dach et al. 2009). We note that using CODE satellite products, rather than IGS ones, is to avoid the possible inhomogeneities of the IGS final products which can degrade the positioning quality of PPP (Teferle et al. 2007).

For data modeling, we applied the absolute phase centers (Schmid et al. 2007), the phase-wind up effects (Wu et al. 1993) and the station displacement models proposed by IERS conventions 2003 (McCarthy and Petit 2004). A cut-off angle of 7° was set for usable measurements and

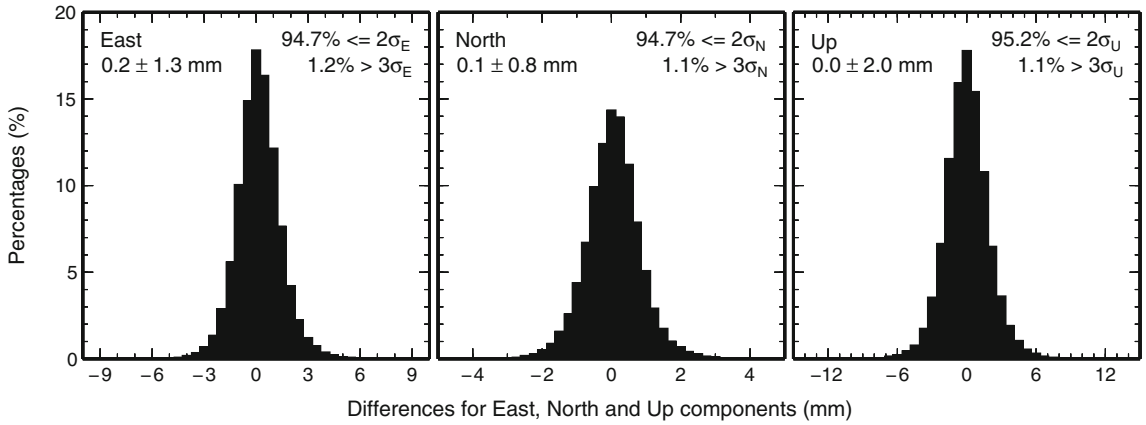

Fig. 1 Magnitude distribution of all position differences between the FCB-based and the IRC-based methods for the East, North and Up components. The *top-left* corner of each subfigure shows the bias and the standard deviation (σ), whereas the *top-right* corner shows the percentages of deviations that are within 2σ, or larger than 3σ ($\sigma_E = 1.3$ mm, $\sigma_N = 0.8$ mm and $\sigma_U = 2.0$ mm). Note that the three subfigures have different horizontal scales

an elevation-dependent weighting strategy was applied to measurements at low elevations. Moreover, we estimated ZTDs every 1 h by applying the global pressure/temperature model and the global mapping function (Kouba 2009), while horizontal tropospheric gradients every 12 h (Bar-Sever et al. 1998). An improved version of PANDA software was used (Shi et al. 2008).

In the following, we used both the FCB-based and IRC-based methods to process these data. We first obtained ambiguity-float daily position estimates by fixing the CODE products. To keep consistency between the CODE products and the PANDA software, we re-estimated the satellite clocks in the FCB-based method by fixing the satellite orbits, the ERPs and the CODE-based ambiguity-float positions. These new satellite clocks were then fixed along with the satellite orbits and the ERPs to estimate the 15-minute mean narrow-lane FCBs using a global network of about 180 stations, most of which located in Europe and North America. Note that double-difference ambiguity resolution was applied to obtain highly accurate satellite-pair FCB estimates (Ge et al. 2005, 2006). Finally, these FCB estimates were used at all 350 stations to fix ambiguities between satellites to integers. On the other hand, in the IRC-based method, the positions of the above 180 stations were fixed to the CODE-based ambiguity-float estimates in order to keep consistency between the reference frames of the FCB-based and IRC-based methods. Based on this, we estimated the IRCs after fixing ambiguities to integers. Finally, these IRC estimates were used at all 350 stations to perform integer ambiguity resolution. Note that integer resolutions were based on the sequential bias-fixing strategy by Ge et al. (2005) under a round-off criterion of 0.2 cycles.

4 Results and discussion

In this section, we present how the FCB-based and IRC-based methods agree in the ambiguity-fixed daily positioning results, including the estimates, the repeatabilities and the RMS statistics against the IGS weekly solutions.

4.1 Position differences

Assessing the differences between the position estimates can directly illustrate to what extent these two methods agree in their positioning results. For each station, we computed ambiguity-fixed position differences between these two methods over 1 year, and removed outliers by a threshold of five times the standard deviations. Finally, less than 0.1% of daily estimates were removed. The RMS statistics of all position differences for all stations are only 1.3, 0.8 and 2.0 mm for the East, North and Up components, respectively. These statistics are well below the formal precisions of 1.8–2.0 mm for the horizontal components and 5.0 mm for the vertical component which were reported on the IGS weekly solutions (Altamimi and Collilieux 2009), implying that the position differences are actually minimal. Furthermore, Fig. 1 shows the magnitude distribution of more than 100,000 position differences for all stations on all days. The biases are only 0.2, 0.1 and 0.0 mm, whereas the standard deviations are 1.3, 0.8 and 2.0 mm for the East, North and Up components, respectively. Hence, the systematic biases between the daily position estimates of these two methods are actually minimal, or even negligible. In addition, about 94.7% in the East, 94.7% in the North and 95.2% in the Up components of all deviations in Fig. 1 are within twice the standard deviations. Therefore, these overall good agreements verify the

theoretical equivalence of the ambiguity-fixed position estimates derived from these two methods.

Nonetheless, large position differences are still present at some stations. For instance, the absolute differences can be up to 10 mm for the East, 6 mm for the North and 20 mm for the Up components. Moreover, 1.2% in the East, 1.1% in the North and 1.1% in the Up components of all differences exceed triple the standard deviations as shown in Fig. 1. Those stations with large position differences usually locate at oceanic islands like Hawaii and Tahiti. Hence, we show the RMS statistics of the position differences over one year for the East component at each station using color scales on a global map (Fig. 2). We can see that, in Europe and North America with relatively dense networks of reference stations, the RMS statistics are well below 1.5 mm, whereas in oceanic areas and Africa with very sparse networks, the RMS statistics are usually over 2.0 mm. This geographical-distribution pattern can also be observed for the North and Up components (not shown here). This finding can be attributed to two aspects. On the one hand, the FCBs cannot be precisely determined or assimilated into clocks over a sparse network because the spatial correlation of errors among the reference stations is very weak. In this case, the difference of separating FCBs from integer ambiguities may amplify the position differences between these two methods. On the other hand, compared with the epoch-wise IRCs, 15- min mean estimates may lead to degraded accuracies of FCBs.

4.2 Position repeatability

Position repeatability can quantitatively reflect the intrinsic positioning quality of these two methods. We generated the position repeatability by deducting a linear model from each station-specific positions over one year and then computing the RMS statistics of the resulting residuals. Outlier rejection was performed by a threshold of five times the standard deviations. Overall, the mean repeatability of all stations is 2.4, 2.2 and 7.7 mm for the FCB-based method, whereas 2.2, 2.3 and 7.6 mm for the IRC-based method for the East, North and Up components, respectively. Hence, the repeatability differences are within only 0.2 mm for all three components which is minimal compared with the repeatability statistics themselves, verifying the theoretical equivalence of the ambiguity-fixed position estimates derived from these two methods.

Nonetheless, these two methods perform geographically differently for the East repeatability. Figure 3 exhibits the East repeatability of the FCB-based method minus that of the IRC-based method for all stations. Hence, positive values in Fig. 3 mean that the IRC-based method outperforms the FCB-based method. We can see that the FCB-based method performs relatively better in Europe, whereas the IRC-based method performs better in oceanic areas like the Pacific and the Indian Ocean. Considering the same models used in both methods, we can attribute this geography-related

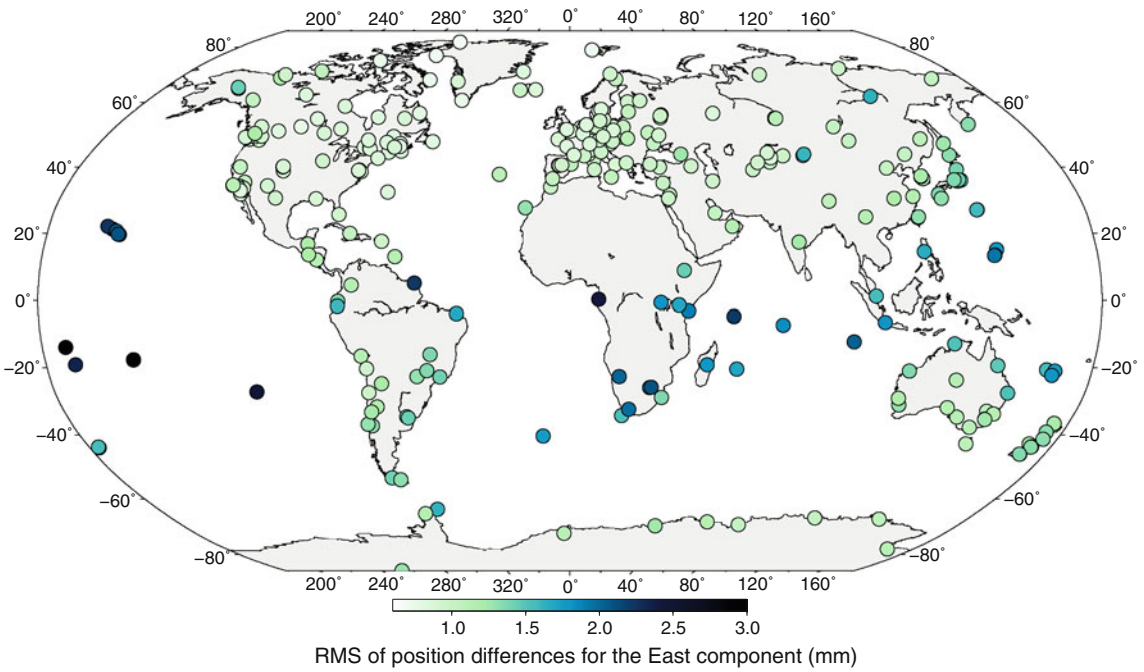

Fig. 2 Geographical distribution of the station-specific RMS statistics of the position differences over 1 year between the two methods for the East component

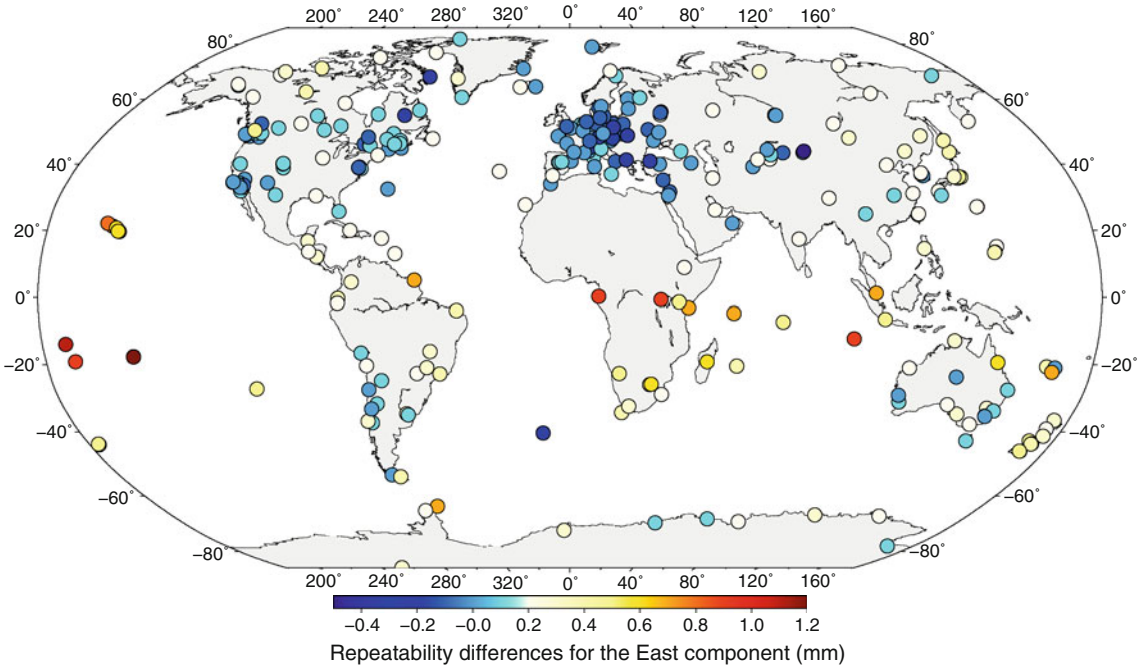

Fig. 3 Geographical distribution of the station-specific position repeatability of the FCB-based method minus that of the IRC-based method for the East component over one year

performance to the reference network density which affects the performance of separating the FCBs from integer ambiguities. In other words, the FCB-based method performs better over a relatively dense network whereas the IRC-based method performs better over a sparse network. However, the IRC-based method can usually perform better by over 0.5 mm, whereas the FCB-based method performs better by less than 0.5 mm, explaining why the IRC-based method overall slightly outperforms the FCB-based method for the East repeatability.

Of particular note, the geographical-distribution pattern of the repeatability differences cannot be observed for the North and Up components (not shown here). Normally, the positioning qualities of the North and Up components are less affected by the integer ambiguity resolution than that of the East component (e.g. Blewitt 1989; Ge et al. 2008), which might explain why we cannot easily observe similar geographical distributions for the North and Up components.

4.3 Comparison with the IGS weekly solutions

In this study, we compared our daily position estimates with the IGS weekly solutions through a 7-parameter Helmert transformation. We removed those position estimates of which the transformed residuals are larger than 15 mm for the horizontal, 30 mm for the vertical components, or five times the standard deviations. RMS statistics of the transformed residuals are used to quantitatively assess the extrinsic positioning quality. Table 1 shows the mean RMS statistics of all days for the ambiguity-float and ambiguity-fixed solutions. In this table, integer ambiguity resolution with the FCB-based method significantly improves the RMS statistics from 3.4, 2.2 and 6.2 mm to 2.0, 2.1 and 5.9 mm for the East, North and Up components, respectively, thereby confirming the results reported by Ge et al. (2008). Likewise, integer ambiguity resolution with the IRC-based method improves the RMS statistics from 3.5, 2.3 and 6.3 mm to 1.9, 2.1 and 5.8 mm. Hence, the RMS difference for the ambiguity-fixed position estimates is within only 0.1 mm for each component which is negligible compared with the RMS statistics themselves, again verifying the theoretical equivalence of the ambiguity-fixed position estimates derived from these two methods.

Table 1 Mean RMS statistics of residuals of the daily ambiguity-float and ambiguity-fixed position estimates against the IGS weekly solutions in 2008

Methods	Ambiguity-float solutions (mm)			Ambiguity-fixed solutions (mm)		
	East	North	Up	East	North	Up
FCB-based	3.4	2.2	6.2	2.0	2.1	5.9
IRC-based	3.5	2.3	6.3	1.9	2.1	5.8

Nonetheless, the IRC-based method performs slightly better for the East component. Figure 4 shows the daily RMS statistics for the East component of the ambiguity-fixed position estimates. Although the RMS statistics of the two methods are close, it is still discernable that the IRC-based statistics

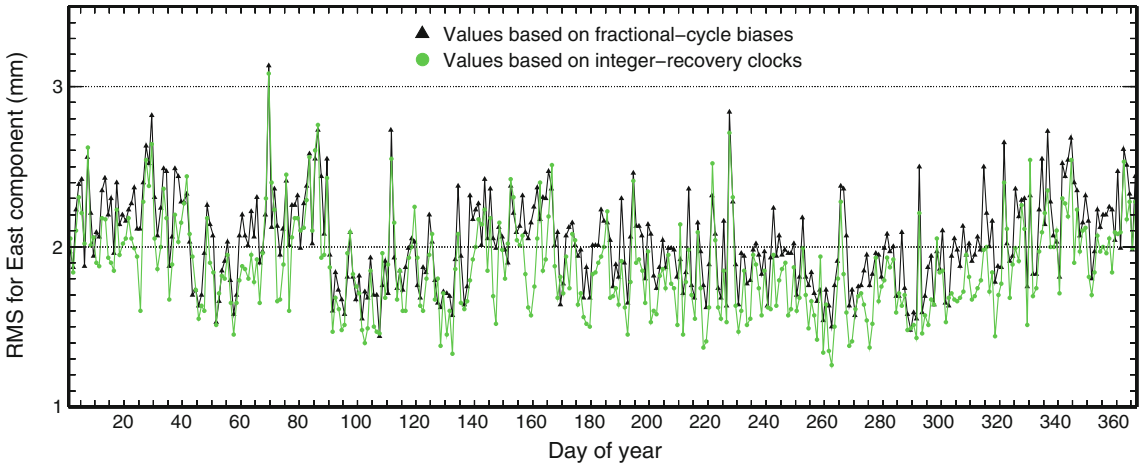

Fig. 4 Daily RMS of residuals of the ambiguity-fixed position estimates against the IGS weekly solutions for the East component in 2008

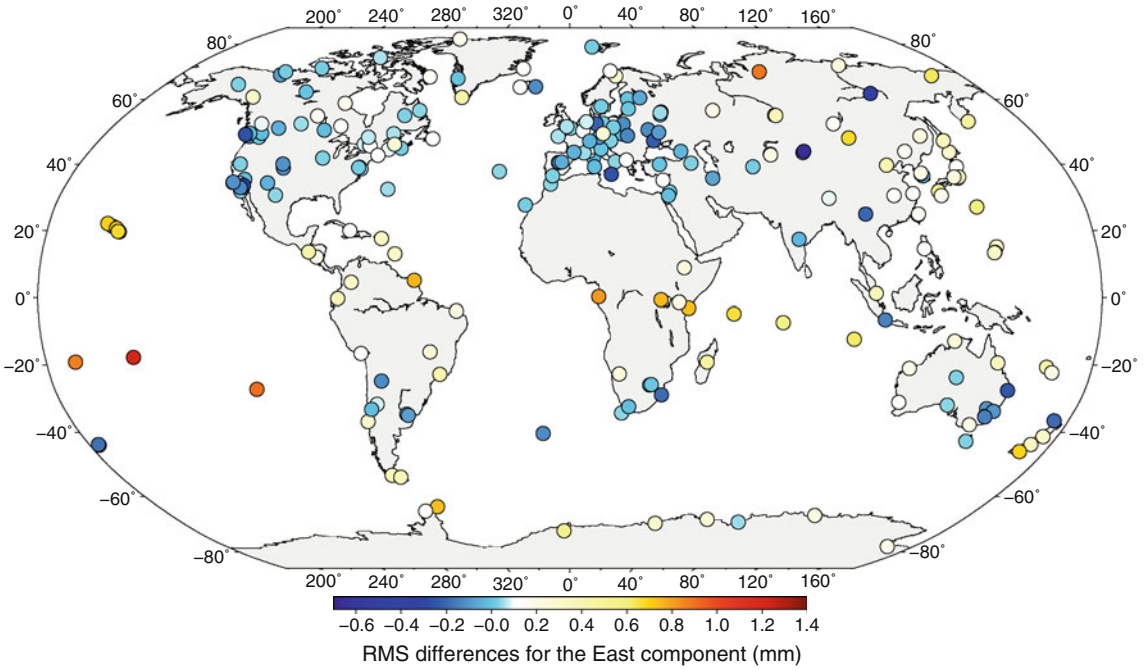

Fig. 5 Geographical distribution of the station-specific RMS for the FCB-based method minus that for the IRC-based method. An RMS is computed over the residuals of ambiguity-fixed position estimates against the IGS weekly solutions for the East component over 1 year

are slightly smaller than the FCB-based statistics on most days. Furthermore, we computed the RMS statistics of the transformed ambiguity-fixed residuals over all days at each station. Figure 5 exhibits the East RMS statistics of the FCB-based method minus those of the IRC-based method for each station. We can see that the FCB-based method performs relatively better in Europe and North America, whereas the IRC-based method performs better in oceanic areas and Africa. However, the IRC-based method can usually perform better by up to 1.4 mm, whereas the FCB-based method performs better by less than 0.7 mm. Hence, the IRC-based method overall slightly outperforms the FCB-based method in the East RMS against the IGS weekly solutions. Additionally, similar to Fig. 3, this geographical-distribution pattern cannot be observed for the North and Up components (not shown here).

5 Conclusions and suggestions

In this study, we theoretically prove the equivalence between the ambiguity-fixed position estimates derived from the two

methods. The FCBs are divided into time-invariant and time-dependent parts. In this manner, we can rigorously model the FCBs, and rigorously derive their impacts on clocks and undifferenced integer ambiguities. Furthermore, we combine these FCBs with clocks and ambiguities under the constraint of minimizing the weighted sum squares of residuals to derive what the FCB and IRC estimates theoretically contain. Finally, by applying these FCB and IRC estimates, we theoretically achieve identical ambiguity-fixed position estimates for these two methods in a single-receiver solution.

In order to verify this equivalence, we compute ambiguity-fixed daily position estimates using both methods with the data from a global network of about 350 reference stations in 2008. The biases between all position estimates are only 0.2, 0.1 and 0.0 mm, whereas the standard deviations of all position differences are only 1.3, 0.8 and 2.0 mm for the East, North and Up components, respectively. Moreover, the differences of position repeatabilities are within only 0.2 mm on average for all three components. The RMS of the position estimates minus those from the IGS weekly solutions for the FCB-based method differs by below 0.1 mm on average for each component from that for the IRC-based method. Hence, the systematic biases between the daily position estimates are actually minimal, or even negligible, and the closeness of the position estimates, repeatabilities and RMS statistics against the IGS weekly solutions overall verify the equivalence of the ambiguity-fixed position estimates derived from the FCB-based and IRC-based methods.

Nonetheless, the different strategies of separating the FCBs from integer ambiguities in these two methods lead to the geographical-distribution patterns of their positioning discrepancy. For instance, for the East component, the station-specific RMS statistics of the position differences are well below 1.5 mm in Europe and North America with relatively-dense networks, whereas usually over 2.0 mm in oceanic areas and Africa with very sparse networks. Moreover, in terms of the East position repeatability and the East RMS statistics against the IGS weekly solutions, the FCB-based method performs slightly better over dense networks, whereas the IRC-based method performs a little better over sparse networks. However, the IRC-based method overall slightly outperforms the FCB-based method for the East component.

Finally, we propose that these two methods should be used in terms of different task constraints. The FCB-based method can conveniently supplement current network solutions as an additional software module, and its FCB determination is compatible with current official clock-generation methods. By contrast, the IRC-based method employs IRCs which are incompatible with current clock products. However, using IRCs is straightforward for the integer ambiguity resolution at a single receiver and the IRC-based method can potentially perform slightly better in practice.

Acknowledgments The authors would like to thank the IGS community for the data and product provision. Thanks also go to Wuhan University for the provision of PANDA software as collaborative research and development. The private communication with Dr Ge from the GeoForschungsZentrum, Potsdam, Germany and Dr Mercier from the Centre National d'Etudes Spatiales, France contributes considerably to this paper. The authors are grateful for the constructive comments by the editor and three reviewers.

Appendix

In general, the GPS pseudorange and carrier-phase measurements on frequency g ($g = 1, 2$) for a station–satellite pair are

$$\begin{cases} P_g = \rho + \dfrac{\kappa}{f_g^2} + \lambda_g b_g + \lambda_g \delta b_g \\ L_g = \rho - \dfrac{\kappa}{f_g^2} + \lambda_g B_g + \lambda_g \delta B_g + \lambda_g N_g \end{cases} \tag{13}$$

where ρ denotes the non-dispersive delay (Ge et al. 2008); λ_g denotes the wavelength; $\dfrac{\kappa}{f_g^2}$ denotes the first-order ionospheric delay; residual measurement errors are ignored and other notations refer to Eq. 1.

By forming the Melbourne–Wübbena combination observable using the pseudorange and carrier-phase observables on both frequencies, we can derive the wide-lane ambiguity as

$$N_1 - N_2 = \frac{L_{mw}}{\lambda_w} - B_1 + B_2 - \delta B_1 + \delta B_2 + \frac{\lambda_n}{\lambda_w}(b_1 + b_2 + \delta b_1 + \delta b_2) \tag{14}$$

where L_{mw} denotes the Melbourne–Wübbena combination measurement in the unit of length; λ_w and λ_n denote the wide-lane and narrow-lane wavelengths, respectively.

Furthermore, by forming the ionosphere-free carrier-phase observable, we can obtain its ambiguity term plus the FCBs as

$$\lambda_3 B_3 + \lambda_3 \delta B_3 + \lambda_3 N_3 = \frac{\lambda_1 f_1^2}{f_1^2 - f_2^2}(B_1 + \delta B_1 + N_1) - \frac{\lambda_2 f_2^2}{f_1^2 - f_2^2}(B_2 + \delta B_2 + N_2) \tag{15}$$

where the subscript "3" is for the ionosphere-free observable, and λ_3, B_3, δB_3 and N_3 are unknown. Substituting N_2 in

Eq. 15 using Eq. 14, we can obtain

$$\lambda_3 B_3 + \lambda_3 \delta B_3 + \lambda_3 N_3 = \frac{\lambda_1 f_1^2}{f_1^2 - f_2^2}(B_1 + \delta B_1 + N_1) - \frac{\lambda_2 f_2^2}{f_1^2 - f_2^2}\left(N_1 - \frac{L_{mw}}{\lambda_w} + B_1 + \delta B_1 - \frac{\lambda_n}{\lambda_w}(b_1 + b_2 + \delta b_1 + \delta b_2)\right) \quad (16)$$

Reformulating Eq. 16, we obtain

$$\lambda_3 B_3 + \lambda_3 \delta B_3 + \lambda_3 N_3 = \lambda_n \left(B_1 + \frac{f_2}{f_1 + f_2}(b_1 + b_2)\right) + \lambda_n \left(\delta B_1 + \frac{f_2}{f_1 + f_2}(\delta b_1 + \delta b_2)\right) + \lambda_n N_1 + \frac{f_2 L_{mw}}{f_1 + f_2} \quad (17)$$

The last term on the right side should be deducted from the corresponding ionosphere-free carrier-phase measurement and thus disappears from Equation 17. Hence, we can assign

$$\begin{cases} B_3 = B_1 + \dfrac{f_2}{f_1 + f_2}(b_1 + b_2) \\ \delta B_3 = \delta B_1 + \dfrac{f_2}{f_1 + f_2}(\delta b_1 + \delta b_2) \\ N_3 = N_1 \end{cases} \quad (18)$$

with $\lambda_3 = \lambda_n$. In this way, we can thus introduce an integer narrow-lane ambiguity into Eq. 1.

References

Altamimi Z, Collilieux X (2009) IGS contribution to the ITRF. J Geod 83(3–4):375–383

Bar-Sever YE, Kroger PM, Borjesson JA (1998) Estimating horizontal gradients of tropospheric path delay with a single GPS receiver. J Geophys Res 103(B3):5019–5035

Blewitt G (1989) Carrier phase ambiguity resolution for the global positioning system applied to geodetic baselines up to 2000 km. J Geophys Res 94(B8):10187–10203

Blewitt G (2008) Fixed point theorems of GPS carrier phase ambiguity resolution and their application to massive network processing: Ambizap. J Geophys Res 113(B12):B12410. doi:10.1029/2008JB005736

Collins P (2008) Isolating and estimating undifferenced GPS integer ambiguities. In: Proceedings of ION national technical meeting, San Diego, US, pp 720–732

Collins P, Lahaye F, Héroux P, Bisnath S (2008) Precise point positioning with ambiguity resolution using the decoupled clock model. In: Proceedings of ION GNSS 21st international technical meeting of the satellite division, Savannah, US, pp 1315–1322

Dach R, Brockman E, Schaer S, Beutler G, Meindl M, Prange L, Bock H, Jäggi A, Ostini L (2009) GNSS processing at CODE: status report. J Geod 83(3–4):353–365

Defraigne P, Bruyninx C (2007) On the link between GPS pseudorange noise and day-boundary discontinuities in geodetic time transfer solutions. GPS Solut 11(4):239–249

Dong D, Bock Y (1989) Global positioning system network analysis with phase ambiguity resolution applied to crustal deformation studies in California. J Geophys Res 94(B4):3949–3966

Dow J, Neilan R, Rizos C (2009) The international GNSS service in a changing landscape of global navigation satellite systems. J Geod 83(3-4):191–198

Gabor MJ, Nerem RS (1999) GPS carrier phase ambiguity resolution using satellite-satellite single difference. In: Proceedings of ION GNSS 12th international technical meeting of the Satellite Division, Nashville, US, pp 1569–1578

Ge M, Gendt G, Dick G, Zhang FP (2005) Improving carrier-phase ambiguity resolution in global GPS network solutions. J Geod 79(1-3):103–110

Ge M, Gendt G, Dick G, Zhang FP, Rothacher M (2006) A new data processing strategy for huge GNSS global networks. J Geod 80(4):199–203

Ge M, Gendt G, Rothacher M, Shi C, Liu J (2008) Resolution of GPS carrier-phase ambiguities in precise point positioning (PPP) with daily observations. J Geod 82(7):389–399

Geng J, Teferle FN, Shi C, Meng X, Dodson AH, Liu J (2009) Ambiguity resolution in precise point positioning with hourly data. GPS Solut 13(4):263–270

Geng J, Meng X, Teferle FN, Dodson AH (2010a) Performance of precise point positioning with ambiguity resolution for 1- to 4-hour observation periods. Surv Rev 42(316):155–165

Geng J, Teferle FN, Meng X, Dodson AH (2010b) Kinematic precise point positioning at remote marine platforms. GPS Solut. doi:10.1007/s10291-009-0157-9

Geng J, Teferle FN, Meng X, Dodson AH (2010c) Towards PPP-RTK: Ambiguity resolution in real-time precise point positioning. Adv Space Res. doi:10.1016/j.asr.2010.03.030

King M, Colemar R, Nguyen LN (2003) Spurious periodic horizontal signals in sub-daily GPS position estimates. J Geod 77(1–2):15–21

Kouba J (2009) Testing of global pressure/temperature (GPT) model and global mapping function (GMF) in GPS analyses. J Geod 83(3–4):199–208

Laurichesse D, Mercier F, Berthias JP, Broca P, Cerri L (2009) Integer ambiguity resolution on undifferenced GPS phase measurements and its application to PPP and satellite precise orbit determination. Navig J Inst Navig 56(2):135–149

McCarthy DD, Petit G (eds) (2004) IERS 2003 conventions. Verlag des Bundes für Kartographie und Geodäsie, Frankfurt am Main, Germany, pp 127

Melbourne WG (1985) The case for ranging in GPS-based geodetic systems. In: Proceedings of first international symposium on precise positioning with the global positioning system, Rockville, US, pp 373–386

Mercier F, Laurichesse D (2008) Zero-difference ambiguity blocking properties of satellite/receiver widelane biases. In: Proceedings of European navigation conference, Toulouse, France

Meyer CD (2000) Matrix analysis and applied linear algebra. Soc Ind Appl Math, Philadelphia, 718

Schmid R, Steigenberger P, Gendt G, Ge M, Rothacher M (2007) Generation of a consistent absolute phase-center correction model for GPS receiver and satellite antennas. J Geod 81(12):781–798

Shi C, Zhao Q, Geng J, Lou Y, Ge M, Liu J (2008) Recent development of PANDA software in GNSS data processing. In: Proceedings of the Society of Photographic Instrumentation Engineers, vol 7285, p 72851S. doi:10.1117/12.816261

Teferle FN, Orliac EJ, Bingley RM (2007) An assessment of Bernese GPS software precise point positioning using IGS final products for global site velocities. GPS Solut 11(3):205–213

Teunissen PJG, Kleusberg A (eds) (1998) GPS for Geodesy, 2nd edn. Springer, Berlin, pp 188–194

Tregoning P, Watson C (2009) Atmospheric effects and spurious signals in GPS analysis. J Geophys Res 114:B09403. doi:10.1029/2009JB006344

Wu JT, Wu SC, Hajj GA, Bertiger WI, Lichten SM (1993) Effects of antenna orientation on GPS carrier phase. Manuscr Geodaet 18(2):91–98

Wübbena G (1985) Software developments for geodetic positioning with GPS using TI-4100 code and carrier measurements. In: Proceedings of first international symposium on precise positioning with the global positioning system, Rockville, US, pp 403–412

Zumberge JF, Heflin MB, Jefferson DC, Watkins MM, Webb FH (1997) Precise point positioning for the efficient and robust analysis of GPS data from large networks. J Geophys Res 102(B3):5005–5017